

Progress in Phased Array Feed Development for Radio Astronomy

BYU

BRIGHAM YOUNG
UNIVERSITY

Brian D. Jeffs, Karl F. Warnick, Jonathan Landon, Michael Elmer
Department of Electrical and Computer Engineering
Brigham Young University, Provo, UT



J. Richard Fisher and Roger Norrod
National Radio Astronomy Observatory
Green Bank, West Virginia

SETI Institute
July 1, 2009

Image courtesy of NRAO/AUI

Single-Pixel Single Reflector Antennas



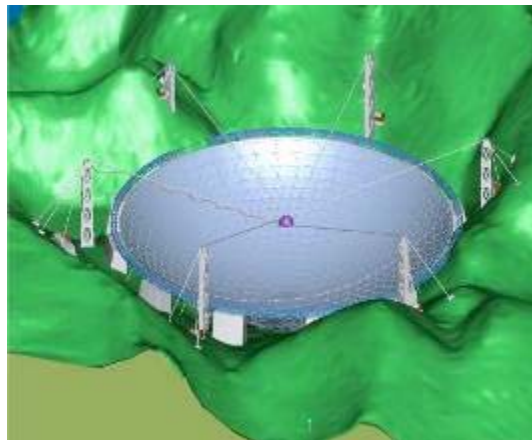
Green Bank Telescope (GBT)

<http://www.astro.virginia.edu/whyastro/gbt+140.jpg>



Arecibo

<http://www.icc.dur.ac.uk/~tt/Lectures/Galaxies/Images/Radio/Arecibo.jpg>



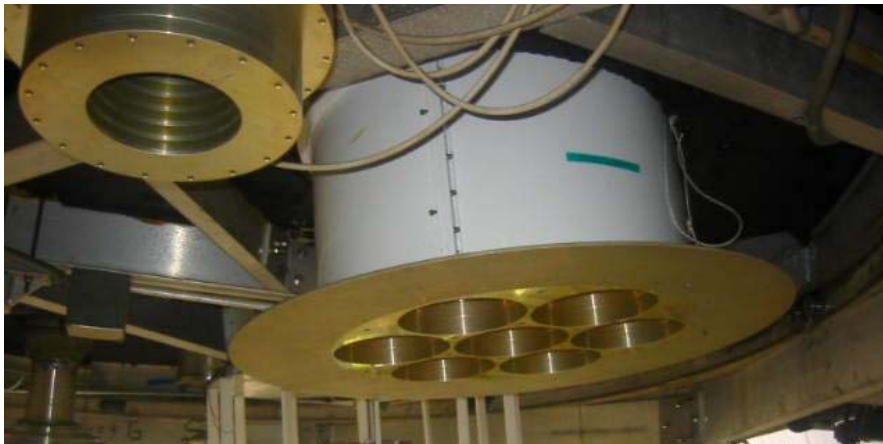
500 meter telescope – China

Under construction

...mature technology, pushed to the limit

Sparse Arrays - Multiple Feeds

- One feed per beam
- Each feed matched to reflector
- Focal plane/field of view not fully sampled --- sparse array



Arecibo L-band feed array (ALFA)

<http://physics.gmu.edu/~lhone/ALFA1.jpg>



Parkes multibeam feed

Image courtesy of Parkes Observatory, ATNF / CSIRO

Array Feed Development Efforts



- Apertif (Astron, The Netherlands)
- PHAD (DRAO, Canada)
- ASKAP (CSIRO, Australia)
- BYU/NRAO Centimeter Band PAF (U.S.)
(Green Bank and Arecibo)



Credit: Tony Willis, NRC - CNRC



Credit: David McClenaghan, CSIRO

Sparse Arrays - Synthesis Imaging



Very Large Array (VLA), Socorro, NM

Image courtesy of NRAO/AUI



Allen Telescope Array (ATA), CA

Image courtesy of SETI Institute, UC Berkeley



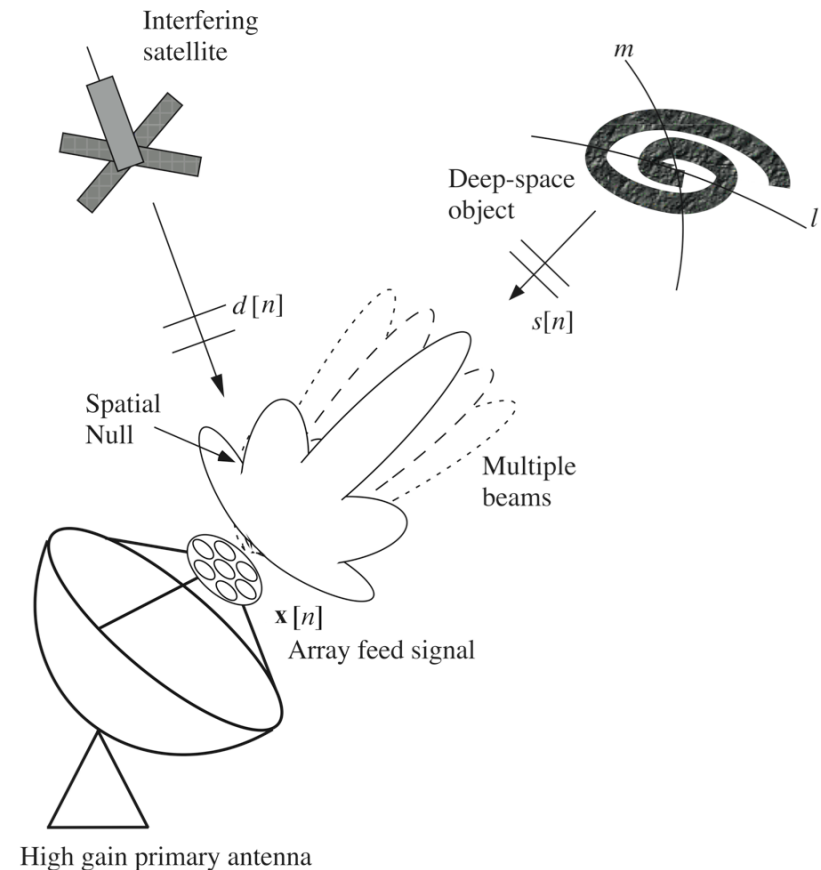
Very Long Baseline Interferometer

Others: Westerbork – The Netherlands
 PAPER Array – Green Bank W.V
 LOFAR – Northern Europe
 LWA – Southwestern U.S.
 ALMA - Chile
 Etc...

The Case for Dense Array Feeds

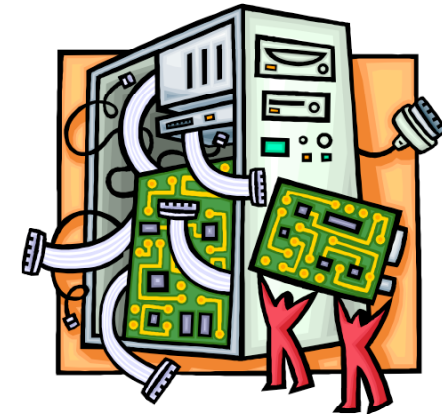
- Primary driver:
 - Increased field of view**
 - Increased survey speed ($\times 10$ to 40).
 - Single dish radio camera imaging.
 - Arbitrarily dense beams.

- Other advantages:
 - Interference cancelation.
 - Increased sensitivity (?).
 - Better off-axis beamshape control than for sparse horn feed arrays.
 - Adaptive illumination pattern, e.g. optimize to spillover noise.



Technical Challenges

- Mutually coupled noise raises T_{rec} .
- Beamforming
 - Stability over time and across beams.
 - Regular calibration required.
 - Beamforming design methods
- System simulation and analysis.
- Hardware complexity and cost.
 - Many receiver channels.
 - EVLA Correlator–like processing per dish!
 - Cryo cooling is difficult.



⇒ Radio astronomy is pushing phased array technology into a new regime!
⇒ New area of R&D for antenna designers...

BYU/NRAO L-Band PAF Development



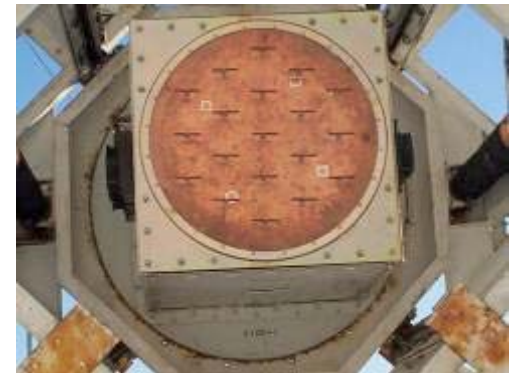
2006:

- 7 element hexagonal single-pol dipole array on 3m reflector
- Array signal processing studies
- RFI mitigation experiments



Nov. 2007:

- 19 element single-pol dipole array on Green Bank 20-Meter Telescope
- Electromagnetically simple elements
- ~1 MHz instantaneous bandwidth
- Real time multichannel data acquisition
- 150 K T_{sys}
- First demonstration of on-reflector PAF



July/August 2008:

- 19 element dipole array
- 33 K LNAs (room temperature)
- 1.3 – 1.7 MHz tunable bandwidth
- *Goal: highest possible sensitivity*
- 66 K T_{sys}





Early radio camera results

Demonstration of PAF image mosaicing on the
Green Bank 20 meter Telescope, July 2008

Single Pointing Image - 3C295



Source: 3C295
Flux density: 21 Jy at 1400 MHz
Observation freq. 1612 MHz
Integration time: 60 sec

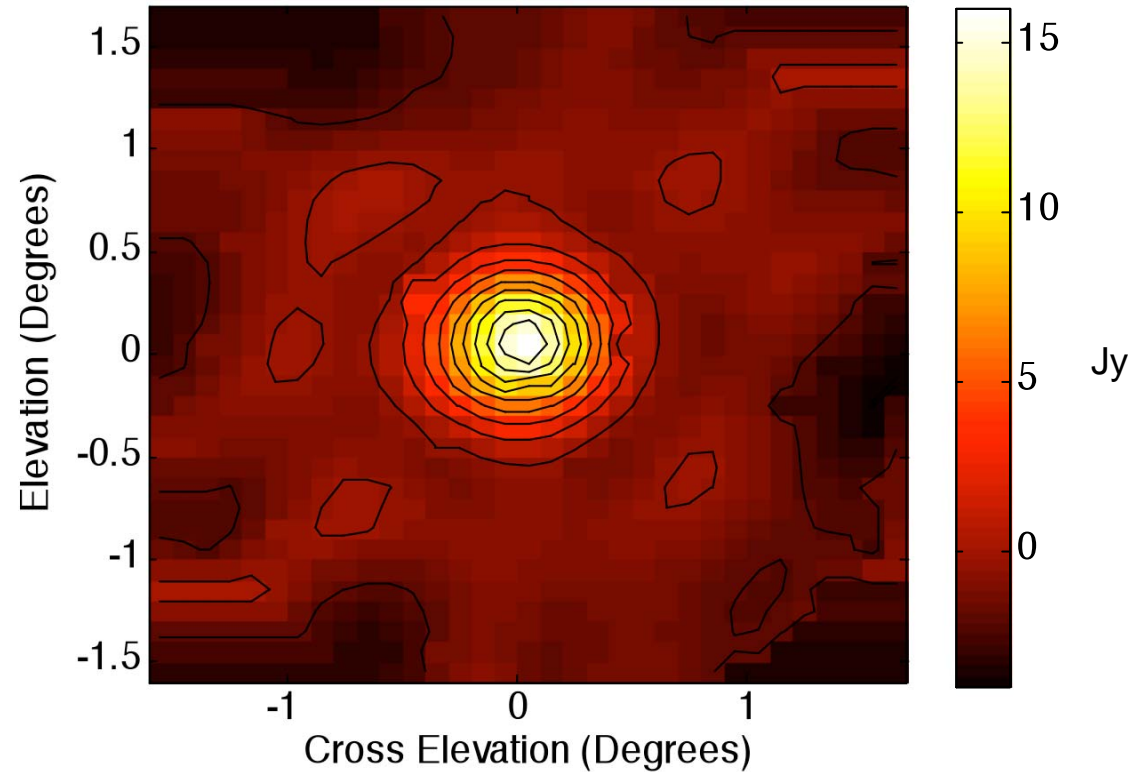
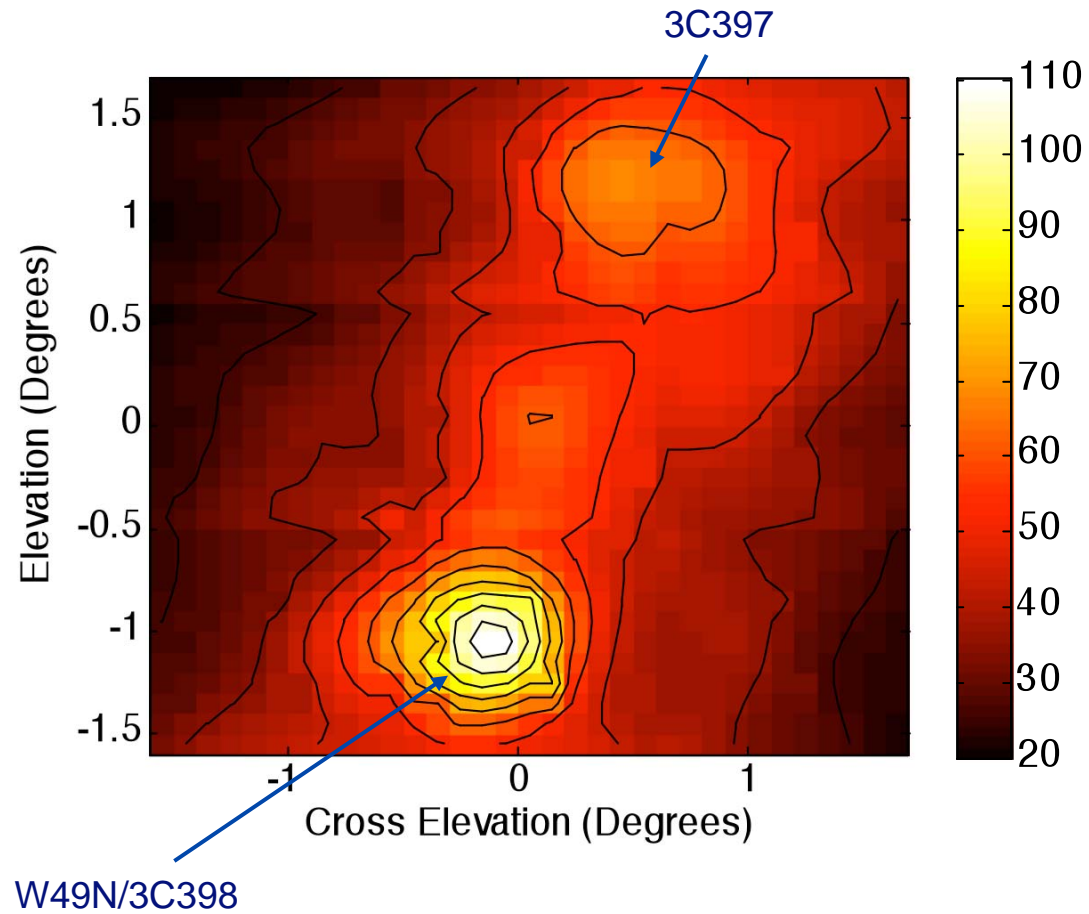


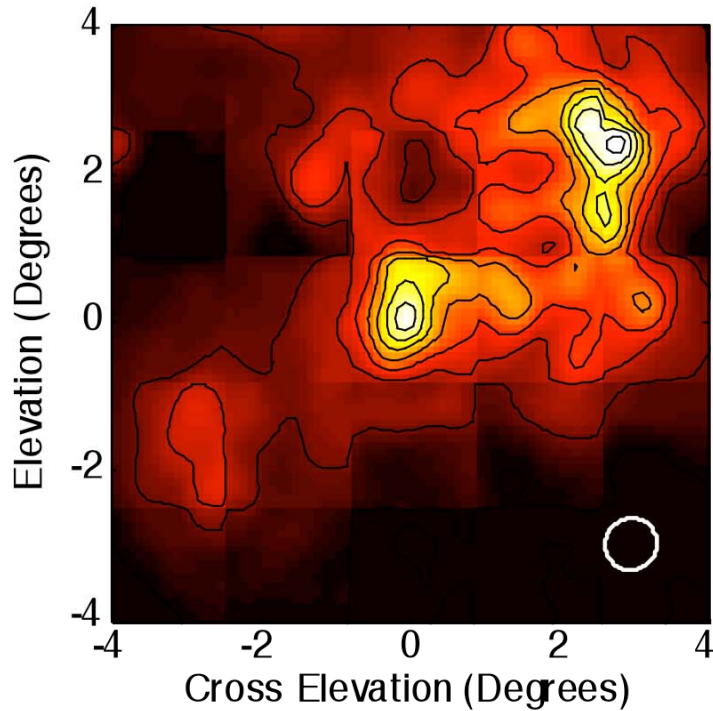
Image Mosaic - W49N Region



1612 MHz
3 x 3 = 9 pointings



Cygnus X Region at 1600 MHz



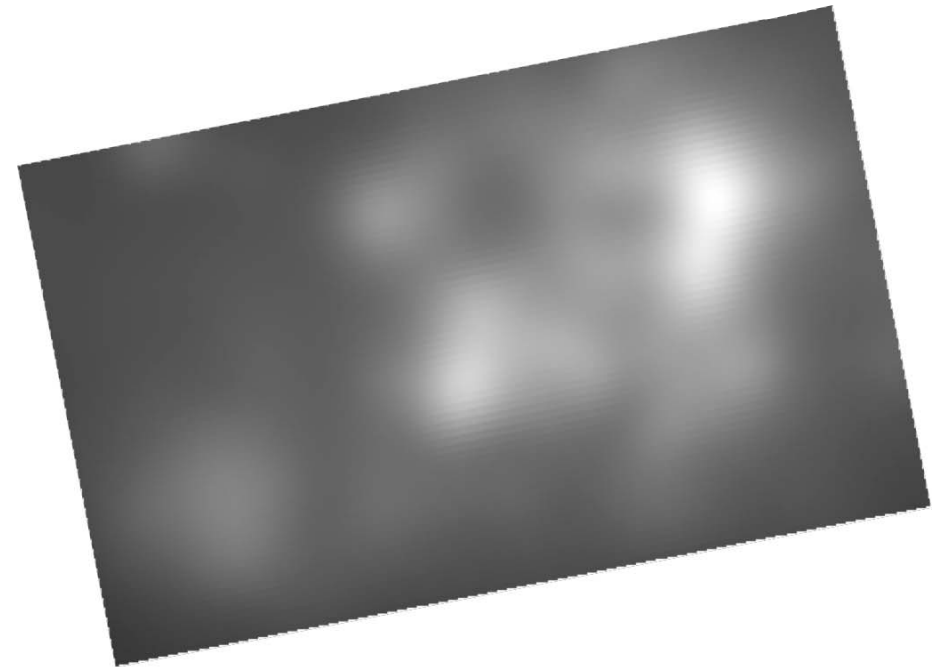
5 x 5 mosaic of PAF pointings.
Circle indicates half power beamwidth.

Required antenna pointings:

Single-pixel feed: ~600

PAF: 25

Imaging speedup: 24x



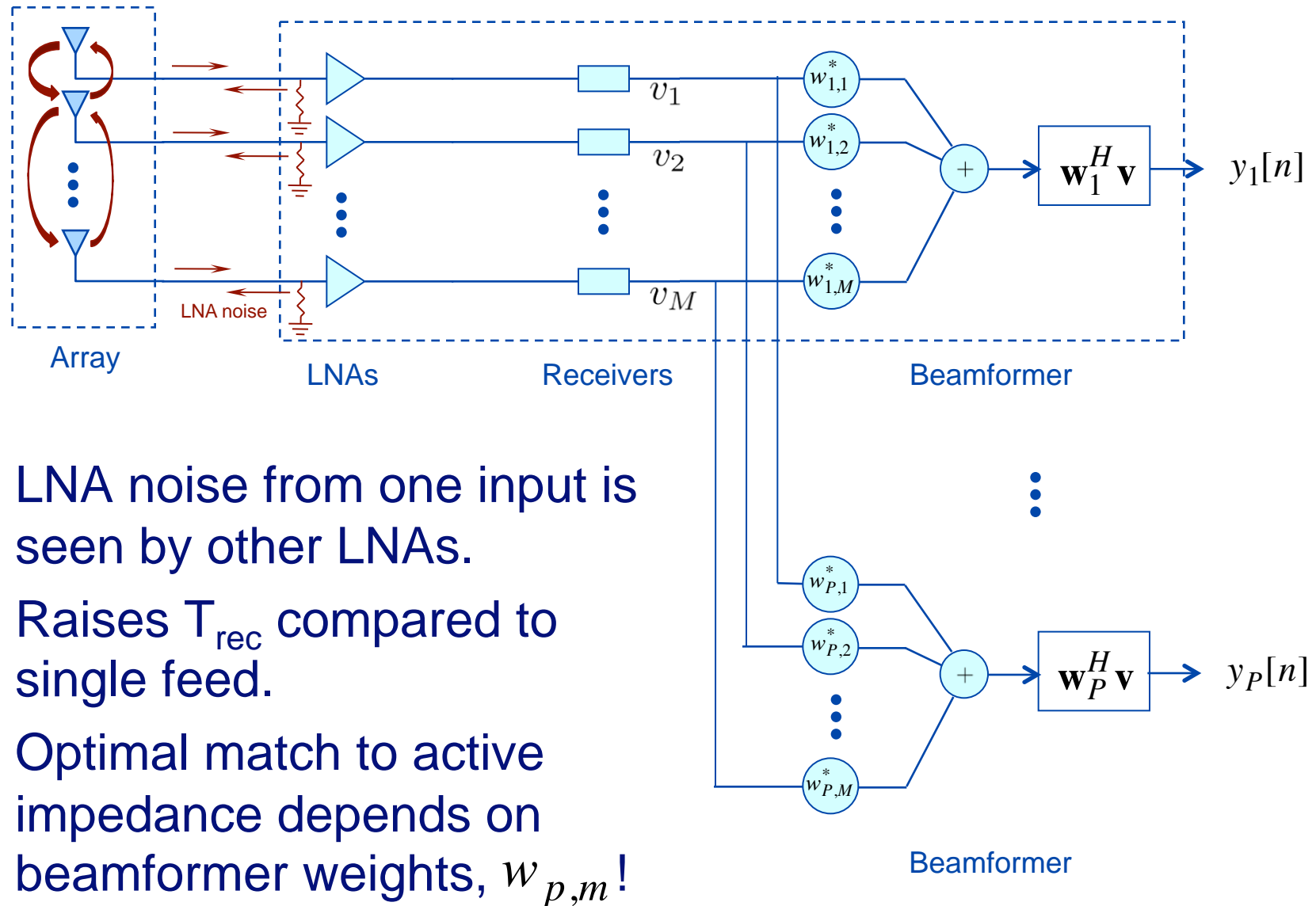
Canadian Galactic Plane Survey
Convolved to 20-Meter beamwidth



Mutually coupled noise

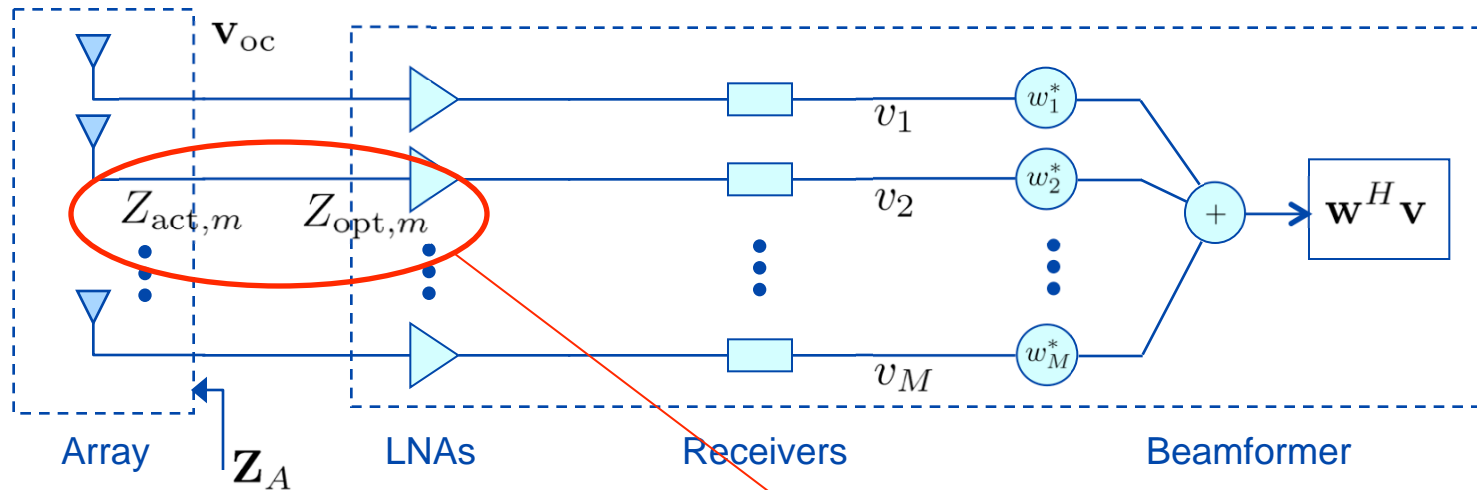
Without careful attention to beam direction dependent matching, T_{rec} increases.

Mutual Coupling Noise Penalty



- LNA noise from one input is seen by other LNAs.
- Raises T_{rec} compared to single feed.
- Optimal match to active impedance depends on beamformer weights, $w_{p,m}$!

Mutual Coupling Noise Penalty



Active impedances [Woestenburg, 2005]:

$$Z_{act,m} = \frac{1}{w_{oc,m}^*} \sum_{n=1}^M w_{oc,n}^* Z_{A,nm}$$

$$T_{rec} = T_{min} + T_0 \frac{\sum_{m=1}^M |w_{oc,m}|^2 R_{n,m} |Z_{act,m}|^2 |Y_{act,m} - Y_{opt,m}|^2}{\sum_{m=1}^M |w_{oc,m}|^2 R_{act,m}}$$

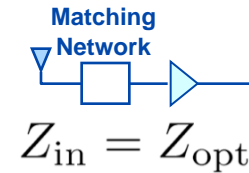
$Z_{act,m} \neq 50 \Omega \Rightarrow 20 K$ increase in effective LNA noise

Noise Matching



Isolated impedance match

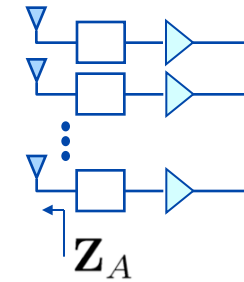
Poor performance for embedded elements



Self impedance match

Performance still poor

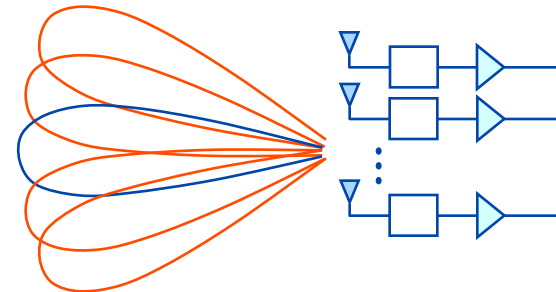
$$Z_{A,mm} = Z_{opt,m}$$



Active impedance match (beam dependent)

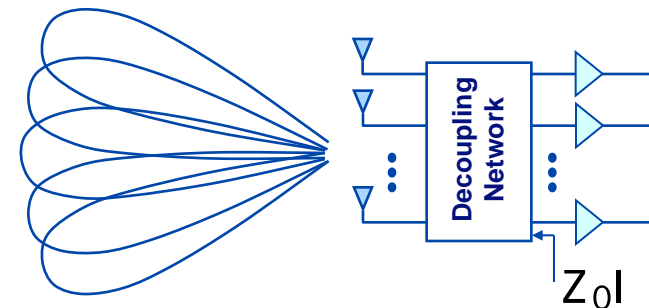
Only maximizes SNR for one beam
 Unstable for PAFs

$$Z_{opt,m} = \frac{1}{w_{oc,m}^*} \sum_{n=1}^M w_{oc,n}^* Z_{A,nm}$$

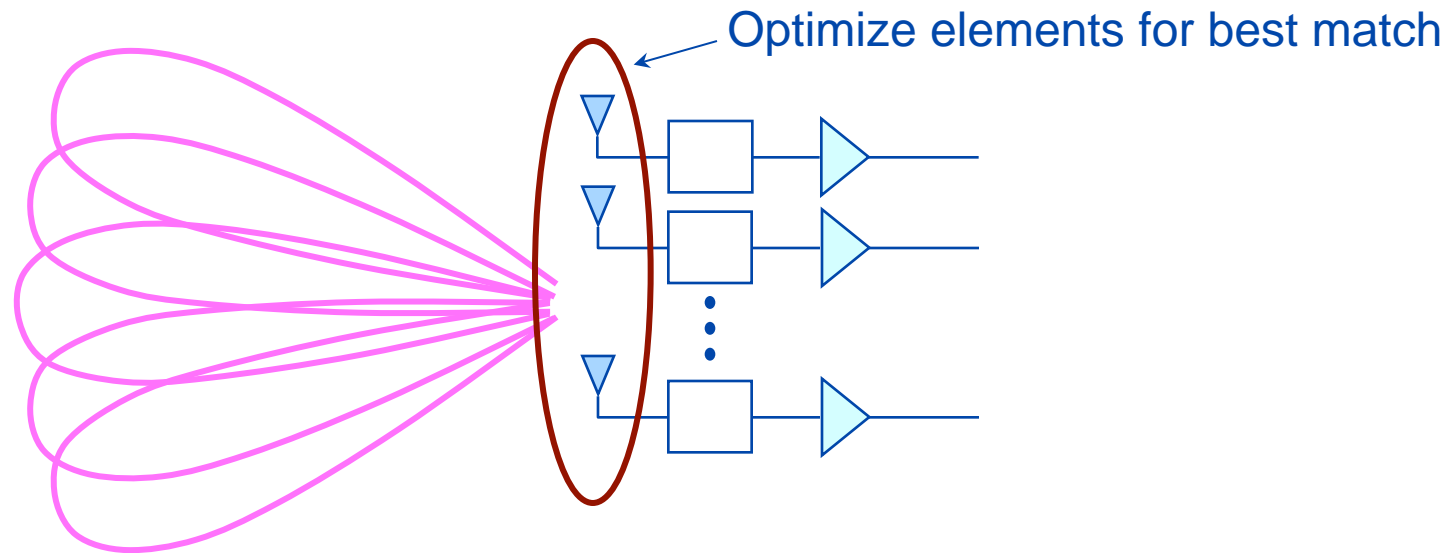


Decoupling network

Optimal for all beams
 Lossy, narrowband



Average Noise Matching Over Beams



- We have good preliminary success with new method.
- Redesign array elements to improve match.
- Minimizes average noise over P beams in a limited field of view.

$$Z_{\text{opt},m} = \frac{\sum_{p=1}^P |w_{\text{oc},m}^p|^2 |Z_{\text{act},m}^p|^2}{\sum_{p=1}^P |w_{\text{oc},m}^p|^2 Z_{\text{act},m}^{p*}}$$

[Warnick, Woestenburg, Belostotski, and Russer, TAP, 2009]



Beamforming

Astronomical PAF arrays pose new challenging
beamformer weight design issues



Candidate Beamforming Modes

- **Fixed beams:** (RF/analog), precalibrated, difficult to design.
- **“Fixed-adaptive” beamforming:** [Jefferies & Warnick, 2007]
 - Calibrate beams using strong point source on steering grid.
 - Optimize sensitivity/SNR for a given pointing direction using maximum SNR beamforming algorithm:

$$\mathbf{R}_{\text{sig}} \mathbf{w} = \lambda_{\text{max}} \mathbf{R}_{\text{noise}} \mathbf{w} \quad \leftarrow \quad (\text{max sensitivity beamformer})$$

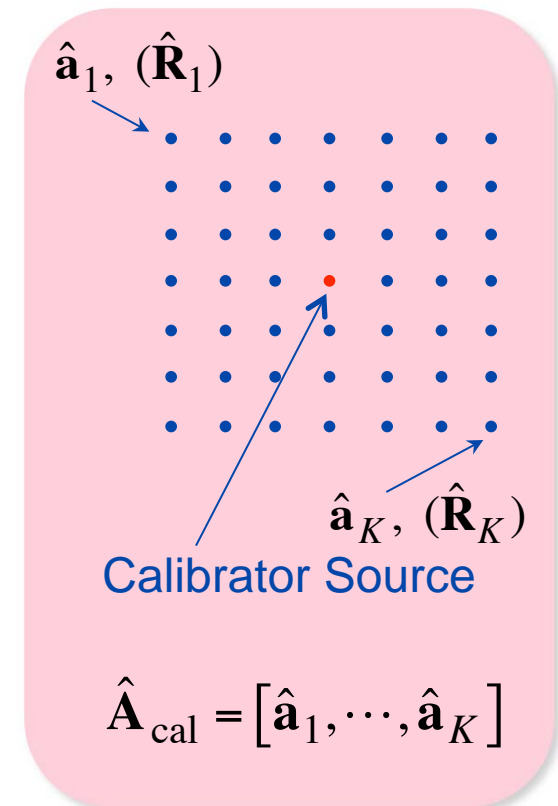
- Periodic adaptation (recalibration) on order of a few days.
- **Slow adaptation:** Irregular updates to noise field changes due to elevation steering. (order of minutes).
- **Fast adaptation:** (Periodic adaptation on order of milliseconds).
 - RFI mitigation: subspace projection, max-SINR algorithms.
 - “Pattern rumble” must be overcome for high sensitivity radiometry.
- **Precomputed deterministic:** Numerically optimized for some desired beamshape property.

-

Array Calibration

- 31×31 raster grid of reflector pointing directions:
 - Centered on calibrator source. e.g. Cas A, Cyg A, Tau A.
 - 10 sec integration per pointing.
 - Acquire array covariance matrices $\hat{\mathbf{R}}_k$ at each pointing.
- One off-pointing per cross elevation row to estimate (2-5 degrees away) $\rightarrow \hat{\mathbf{R}}_{\text{noise}}$
- k th calibration steering vector is estimated by:

$$\hat{\mathbf{a}}_k = \hat{\mathbf{R}}_{\text{noise}} \mathbf{u}_{\text{max},k}, \quad \hat{\mathbf{R}}_k \mathbf{u}_{\text{max},k} = \lambda_{\text{max}} \hat{\mathbf{R}}_{\text{noise}} \mathbf{u}_{\text{max},k}$$
- Calibrations stable for days.
- Cannot calibrate beyond first couple of sidelobes.

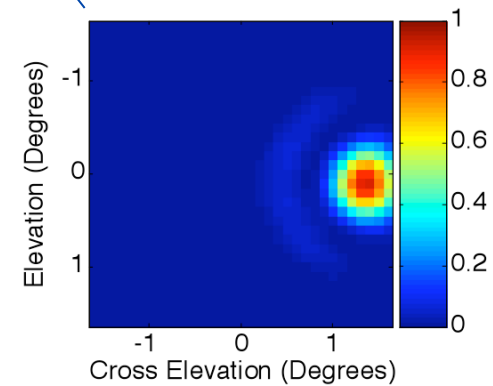
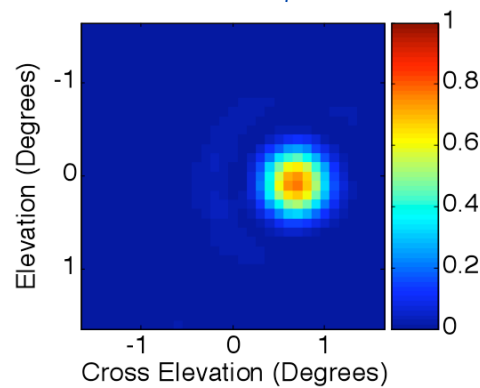
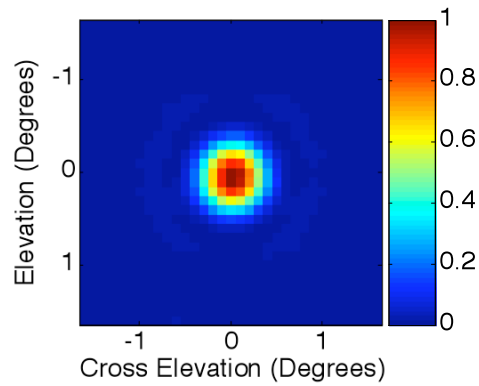
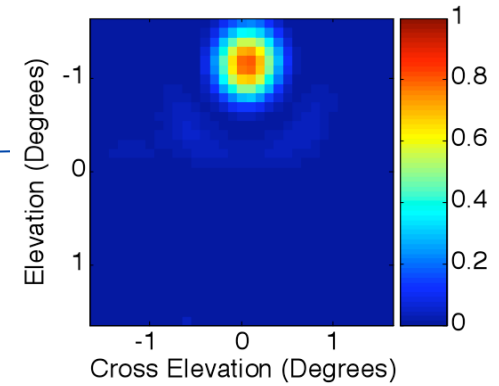
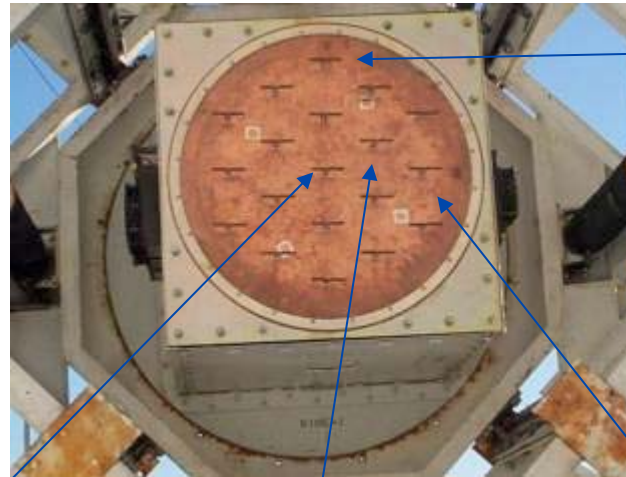


Array output voltage correlation matrix:
$$\mathbf{R}_k = E\{\mathbf{v}\mathbf{v}^H\} = \mathbf{R}_{\text{sig},k} + \underbrace{\mathbf{R}_{\text{sp}} + \mathbf{R}_{\text{rec}} + \mathbf{R}_{\text{sky}} + \mathbf{R}_{\text{loss}}}_{\mathbf{R}_{\text{noise}}}$$

Element Patterns



Source: Cas A, 1612 MHz
0.1 degree pointing grid

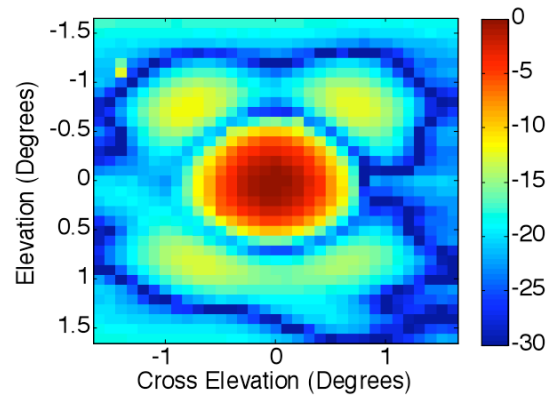


Scale: Linear relative to center element max

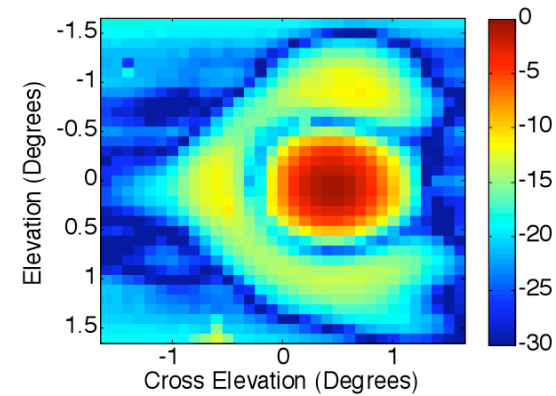
Maximum Sensitivity Beam Patterns



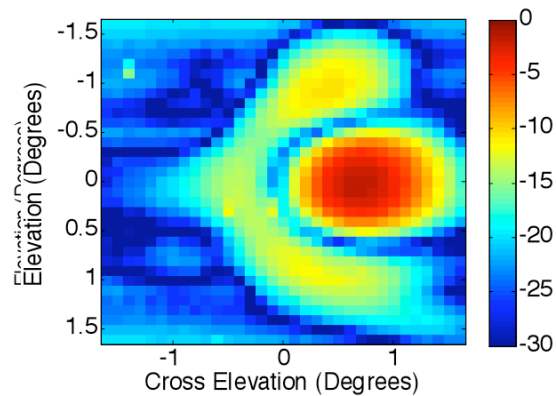
Boresight



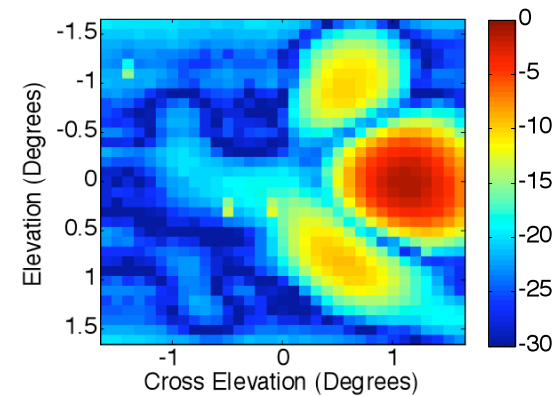
0.4°



0.8°

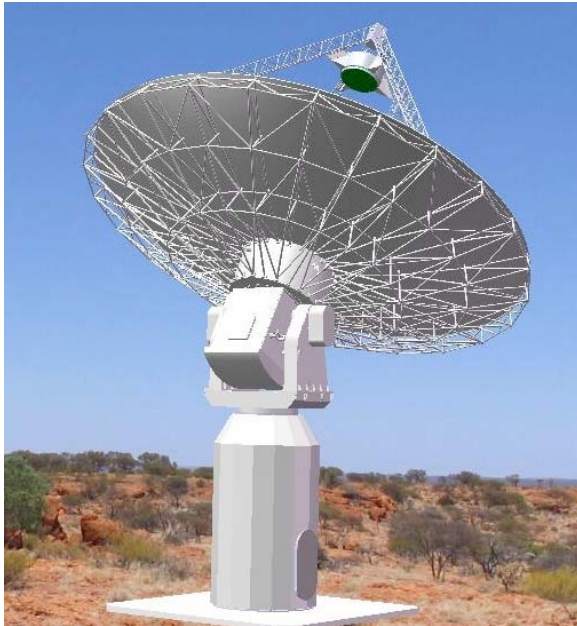


1.2°

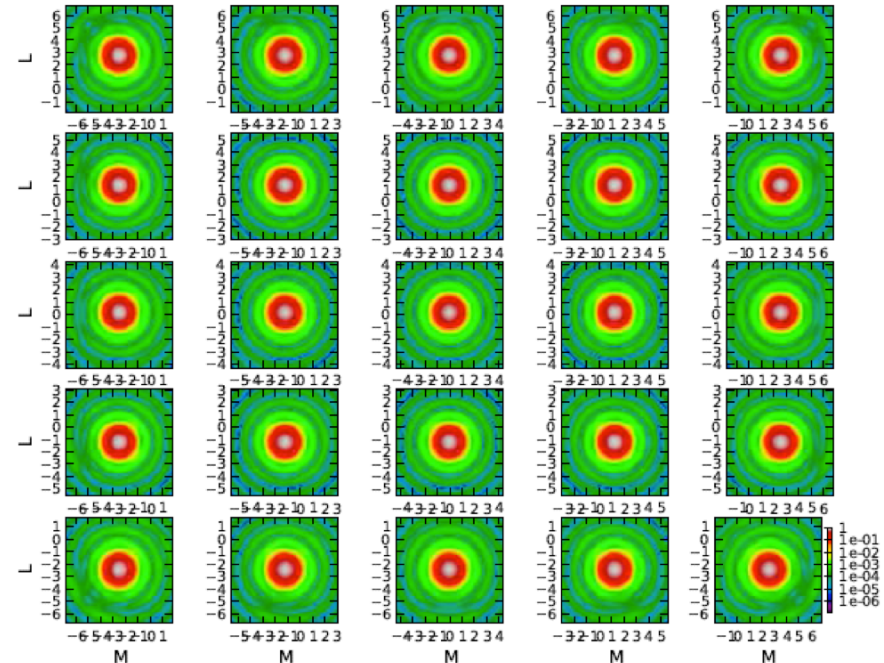


Scale: dB relative to boresight beam max

Beampattern Consistency Solutions



ASKAP dish Credit: CSIRO, Ross Forsyth

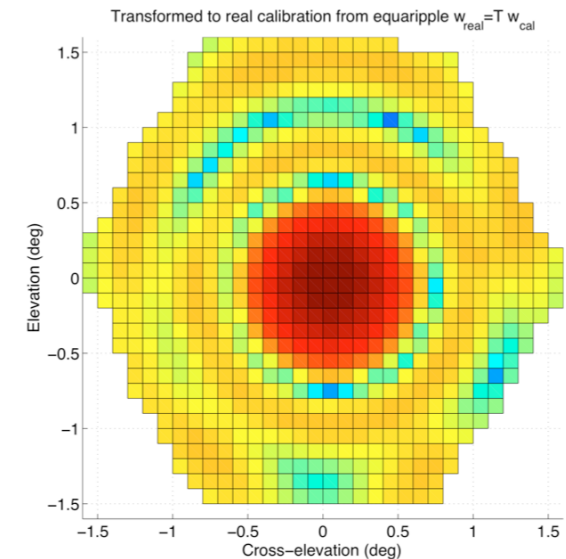
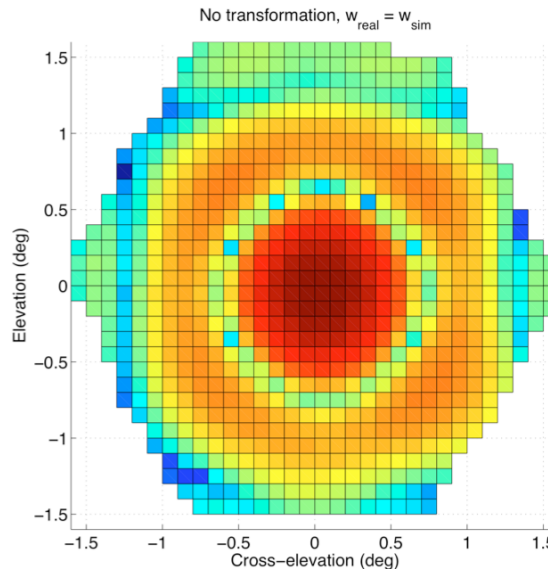
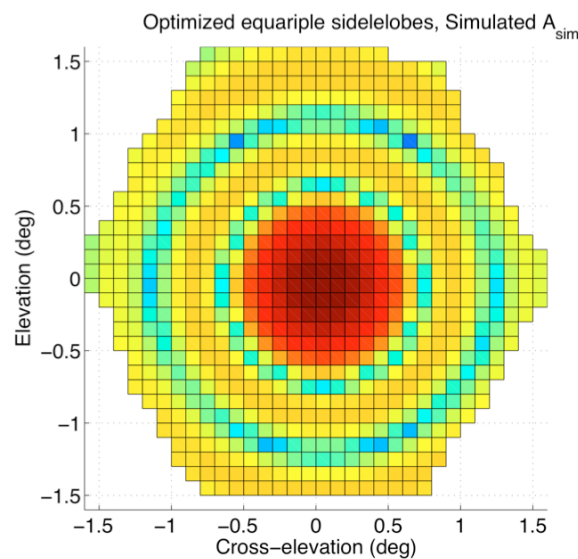


Credit: Tony Willis, DRAO, NRC - CNRC

- Consistency with dish pointing:
 - Three-axis instrument (ASKAP)
 - Equatorial mount (APERTIF, Westerbork).
 - Beampattern optimized deterministic weights.

- Consistency across beams:
 - Response constraints in max sensitivity: LCMV beamformer
 - Beampattern optimized deterministic weights. e.g. (above) Tony Willis, CALIM09. simulated beampattern designs.

Problems with deterministic designs



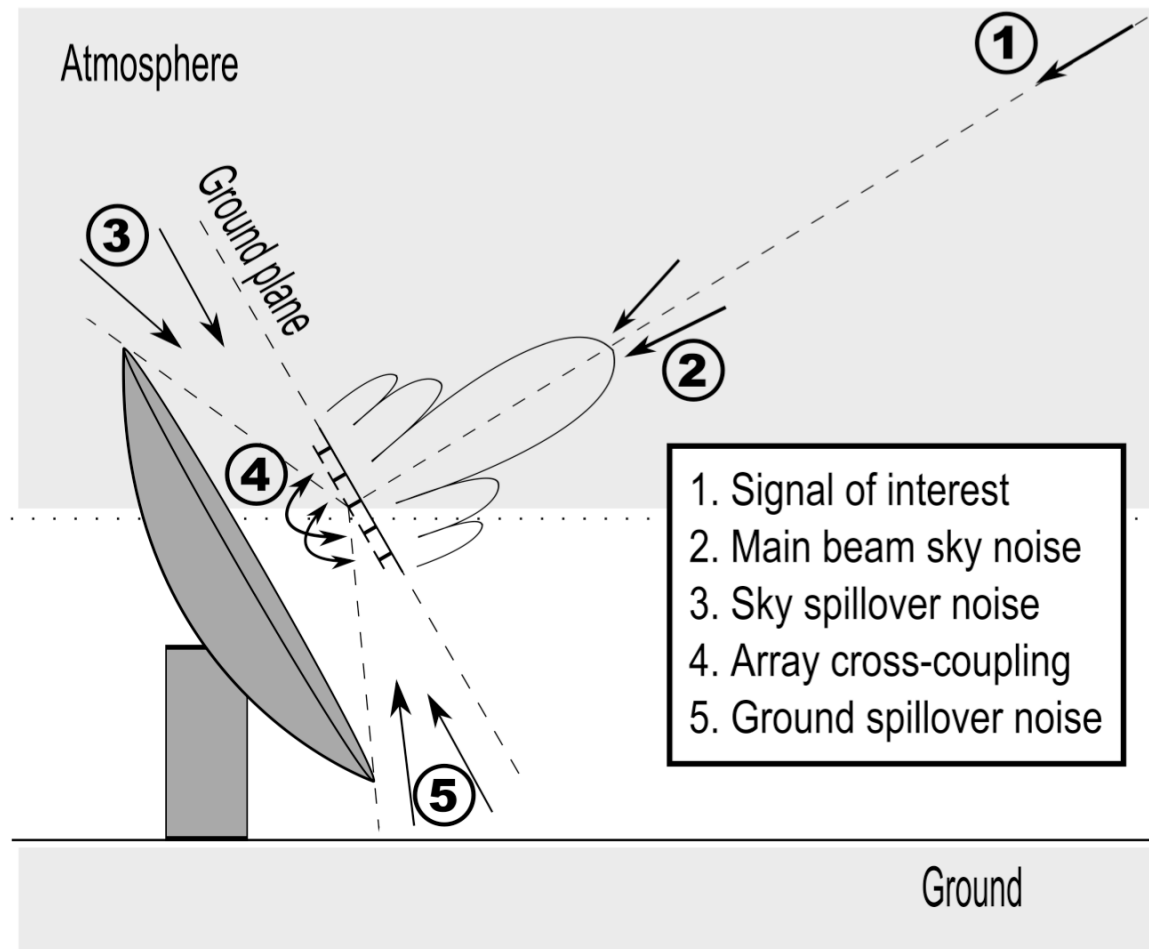
- Best array–dish simulations only match reality qualitatively.
- Calibrations are only available on a small grid in field of view.
- Optimized patterns over large simulated response grids do not migrate to real array.

- Solution: Calibration correction:

$$\mathbf{w}_{real} = \mathbf{T}_{map} \mathbf{w}_{sim}$$

$$\mathbf{T}_{map} = \arg \min_{\mathbf{T}} \left| \mathbf{A}_{cal} - \mathbf{T} \mathbf{A}_{sim} \right|_{Fro}^2$$

Elevation Dependent Noise Covariance

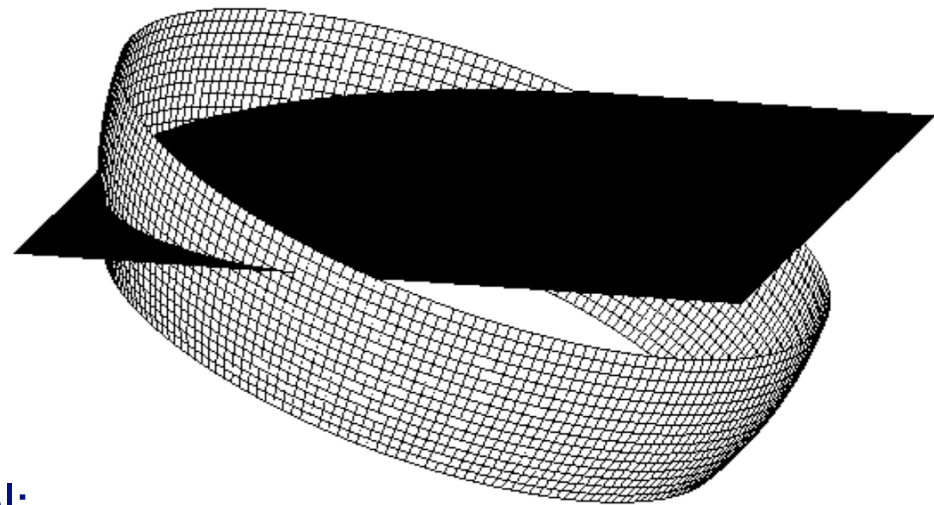


Spillover region is numerically modeled as a grid of point sources. As the dish is tipped, a portion of the spillover region passes through the sky/ground plane and sees the colder sky.

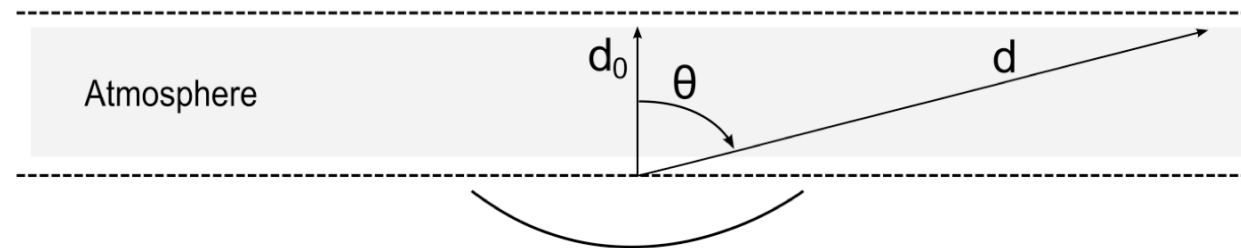
Spillover and Sky Noise Models



- Spillover noise model:



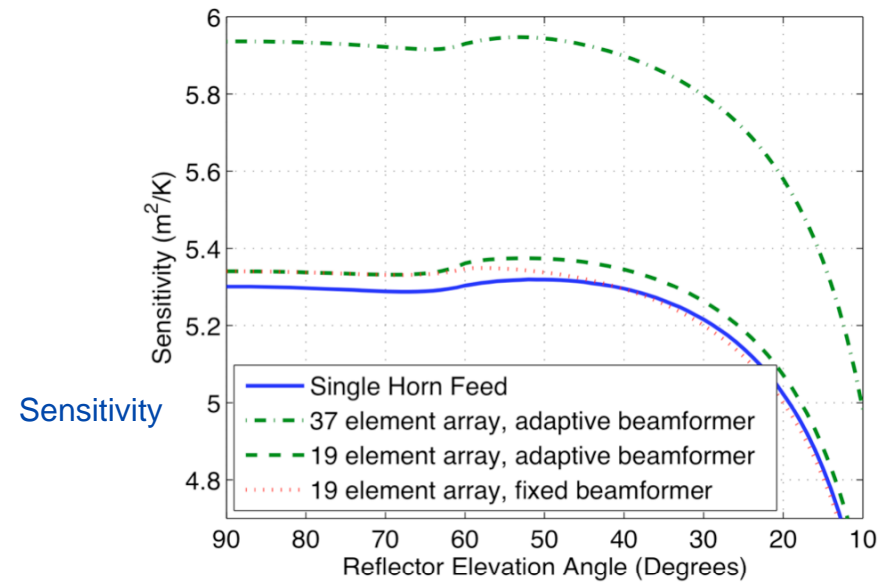
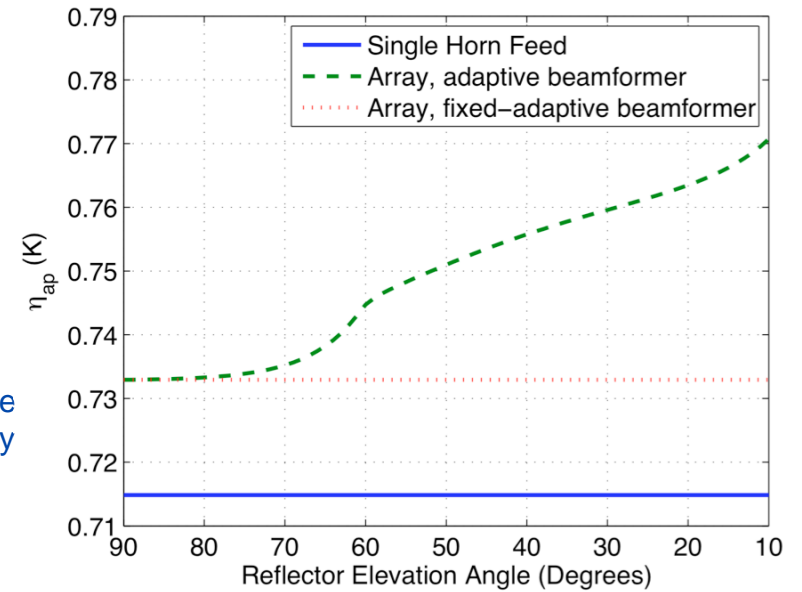
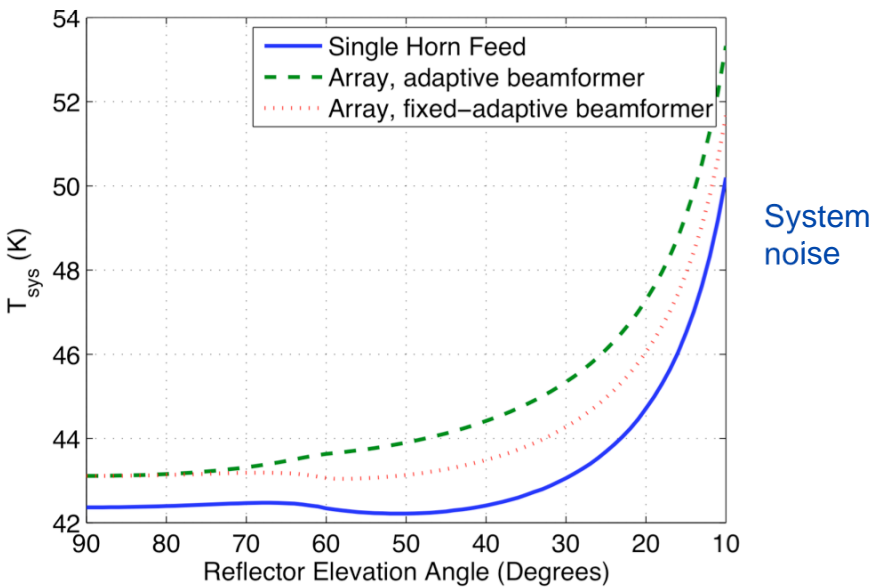
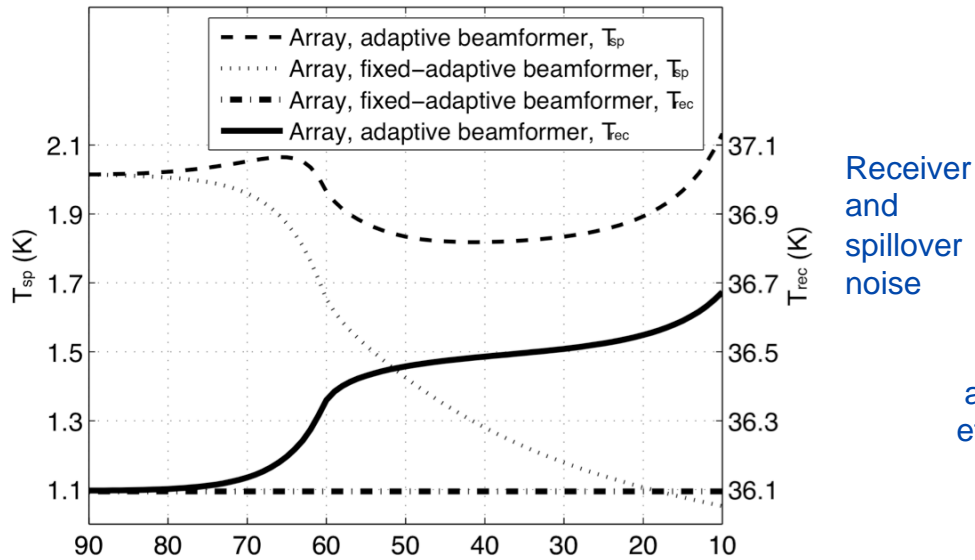
- Main beam sky noise model:



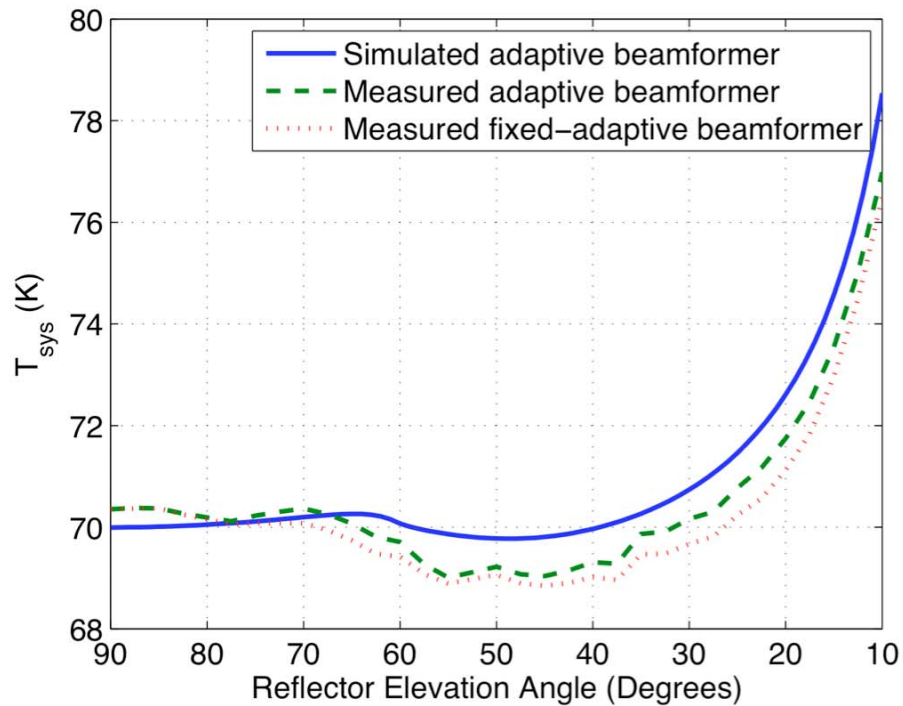
- Total noise model:

$$\mathbf{R}_{\text{noise}} = \mathbf{R}_{\text{rec}} + \mathbf{R}_{\text{sp}} + \mathbf{R}_{\text{mb}}, \quad T_{\text{sys}} = T_{\text{iso}} \frac{\mathbf{w}^H \mathbf{R}_{\text{noise}} \mathbf{w}}{\mathbf{w}^H \mathbf{R}_{\text{iso}} \mathbf{w}}$$

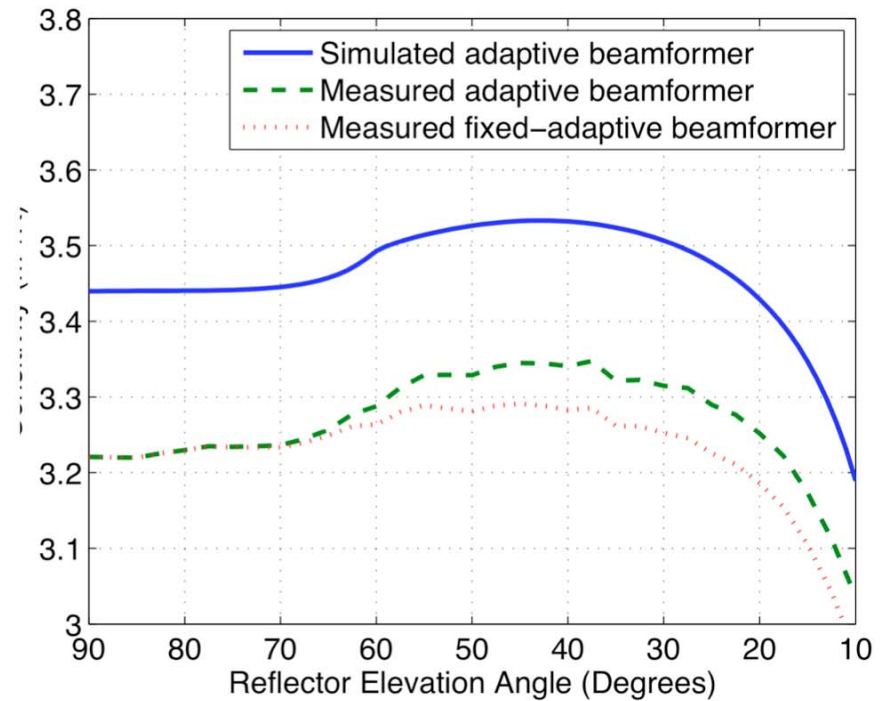
Simulation Results



20m dish Real Data Comparisons



System Temperature



System Sensitivity



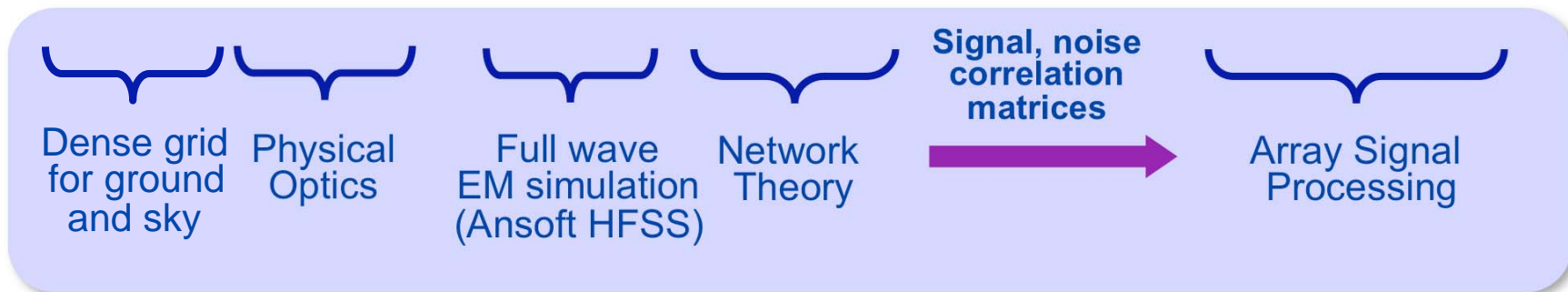
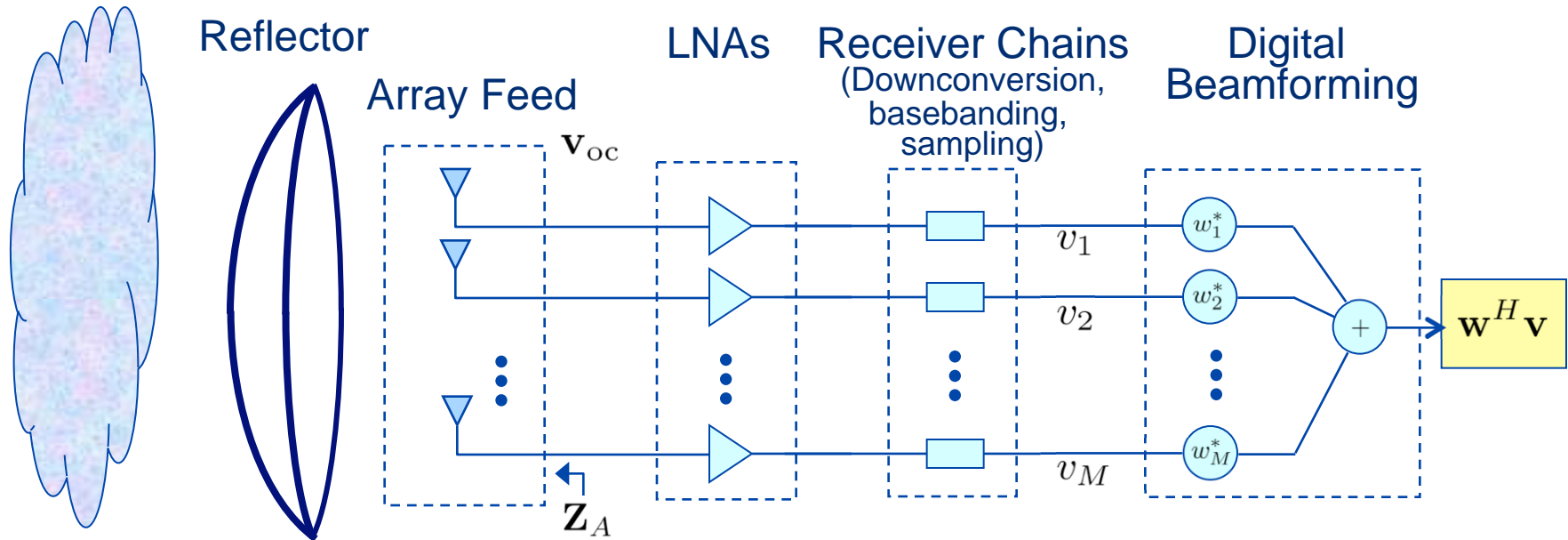
PAF analysis and modeling

System performance metrics are proposed and detailed analytical models are developed

System Model



Noise Field



Beam Sensitivity and Efficiencies



Sensitivity:

$$\frac{A_e}{T_{\text{sys}}} = \frac{k_b B}{S^{\text{sig}}} \text{SNR} \quad (\text{m}^2/\text{K})$$

$$\frac{A_e}{T_{\text{sys}}} = \frac{2k_b}{10^{-26} F^{\text{sig}}} \frac{\mathbf{w}^H \mathbf{R}_{\text{sig}} \mathbf{w} - \mathbf{w}^H \mathbf{R}_{\text{noise}} \mathbf{w}}{\mathbf{w}^H \mathbf{R}_{\text{noise}} \mathbf{w}} \quad \begin{array}{l} \leftarrow P_{\text{sig}} \\ \leftarrow P_{\text{noise}} \end{array}$$

$$= \frac{\eta_{\text{rad}} \eta_{\text{ap}} A_p}{T_{\text{sky}} + \underbrace{\eta_{\text{rad}} (1 - \eta_{\text{sp}}) T_g}_{T_{\text{sp}}} + \underbrace{(1 - \eta_{\text{rad}}) T_a}_{T_{\text{loss}}} + \underbrace{T_{\text{min}} / \eta_n}_{T_{\text{rec}}}}$$

Efficiencies:

Aperture efficiency: $\eta_{\text{ap}} = \frac{k_b T_{\text{iso}}}{A_p (F^{\text{sig}}/2)} \frac{\mathbf{w}^H \mathbf{R}_{\text{sig}} \mathbf{w}}{\mathbf{w}^H \mathbf{R}_{\text{iso}} \mathbf{w}}$

Spillover efficiency: $\eta_{\text{sp}} = 1 - \frac{\mathbf{w}^H \mathbf{R}_{\text{sp}} \mathbf{w}}{\mathbf{w}^H \mathbf{R}_{\text{iso}} \mathbf{w}}$

Noise correlation for perfect "sky"

Radiation efficiency: $\eta_{\text{rad}} = \frac{\mathbf{w}^H \mathbf{R}_{\text{iso}} \mathbf{w}}{\mathbf{w}^H (\mathbf{R}_{\text{iso}} + \mathbf{R}_{\text{loss}}) \mathbf{w}}$

Noise matching efficiency: $\eta_n = \frac{T_{\text{min}}}{T_{\text{iso}}} \frac{\mathbf{w}^H \mathbf{R}_{\text{iso}} \mathbf{w}}{\mathbf{w}^H \mathbf{R}_{\text{rec}} \mathbf{w}}$

Consistent with IEEE Standard Definition of Terms for Antennas

Warnick and Jeffs, "Efficiencies and system temperature for a beamforming array," AWPL, 2008]

Cold Sky/Warm Absorber Setup



Array Y Factor Measurement



$$\begin{aligned} \text{Absorber: } \mathbf{R}_{\text{hot}} &= \frac{T_{\text{hot}}}{T_{\text{iso}}} \mathbf{R}_{\text{iso}} + \mathbf{R}_{\text{rec}} + \mathbf{R}_{\text{loss}} \\ \text{Sky: } \mathbf{R}_{\text{cold}} &= \frac{T_{\text{cold}}}{T_{\text{iso}}} \mathbf{R}_{\text{iso}} + \mathbf{R}_{\text{rec}} + \mathbf{R}_{\text{loss}} \end{aligned}$$



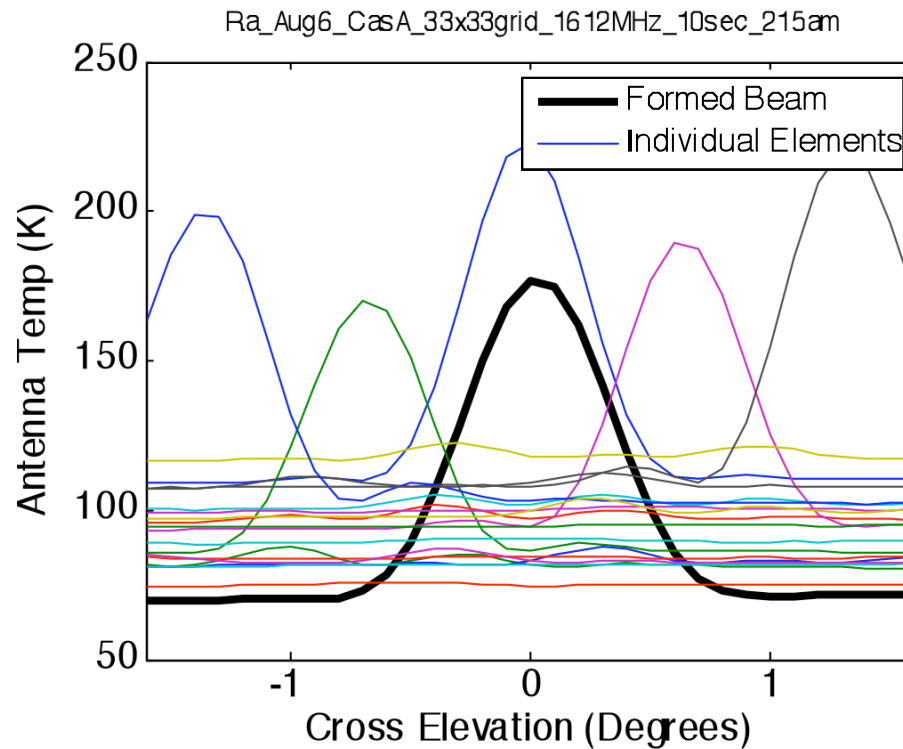
$$\begin{aligned} \mathbf{R}_{\text{iso}} &= \frac{T_{\text{iso}}}{T_{\text{hot}} + T_{\text{cold}}} (\mathbf{R}_{\text{hot}} - \mathbf{R}_{\text{cold}}) \\ \mathbf{R}_{\text{rec}} + \mathbf{R}_{\text{loss}} &= \frac{T_{\text{hot}} \mathbf{R}_{\text{cold}} - T_{\text{cold}} \mathbf{R}_{\text{hot}}}{T_{\text{hot}} - T_{\text{cold}}} \end{aligned}$$

Isotropic noise response allows efficiency and system temperature to be determined from on/off source pointings:

$$\eta_{\text{ap}} = \frac{k_b T_{\text{iso}} B}{A_p S^{\text{sig}}} \frac{\mathbf{w}^H \mathbf{R}_{\text{sig}} \mathbf{w}}{\mathbf{w}^H \mathbf{R}_{\text{iso}} \mathbf{w}}$$

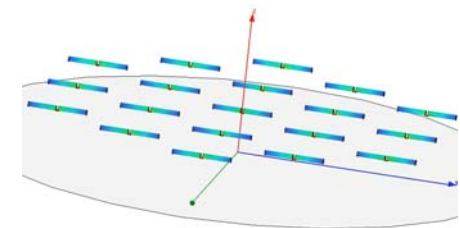
$$T_{\text{sys}} / \eta_{\text{rad}} = T_{\text{iso}} \frac{\mathbf{w}^H \mathbf{R}_{\text{noise}} \mathbf{w}}{\mathbf{w}^H \mathbf{R}_{\text{iso}} \mathbf{w}}$$

On-Reflector Results (July 2008)



Cas A scan
1612 MHz

	Center Element	Formed Beam	Model (FEM)
Sensitivity:	2 m ² /K	3.3 m²/K	3.7 m ² /K
T _{sys} :	101 K	66 K	69 K
Efficiency:	64%	69%	81%



System Noise Budget

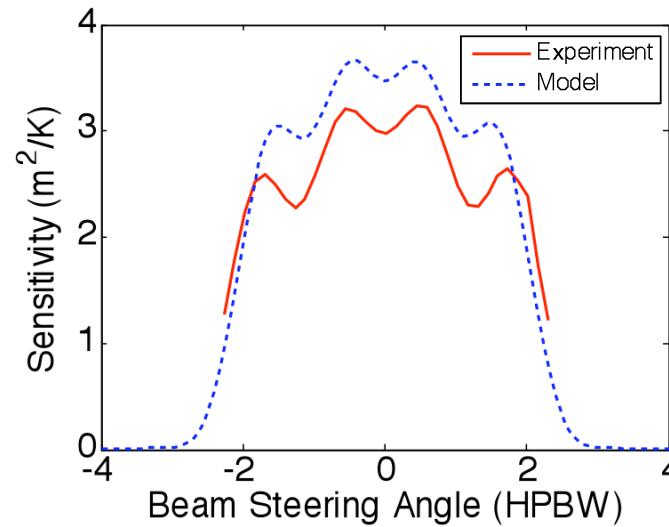
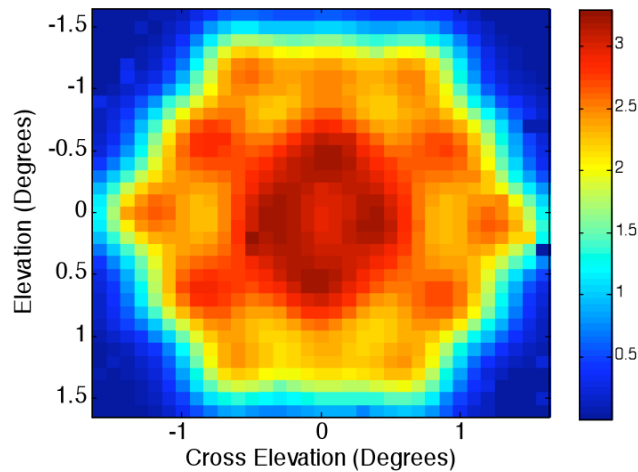


	Measured	Model	
LNA T_{\min}	33 K	33 K	
Mutual coupling	20 K	23 K	← Noise matching efficiency 60%
Spillover	5 K	5 K	
Sky	3 K	3 K	
Loss	5 K	5 K	
T_{sys}:	66 K	69 K	

Beam Sensitivity, Efficiency, T_{sys}

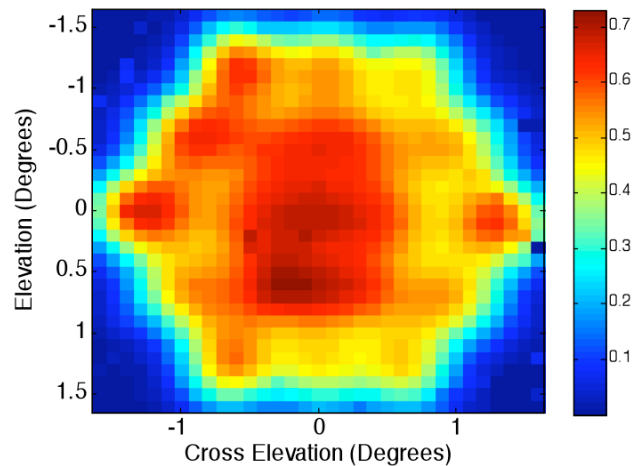


Beam Sensitivity (m^2/K)

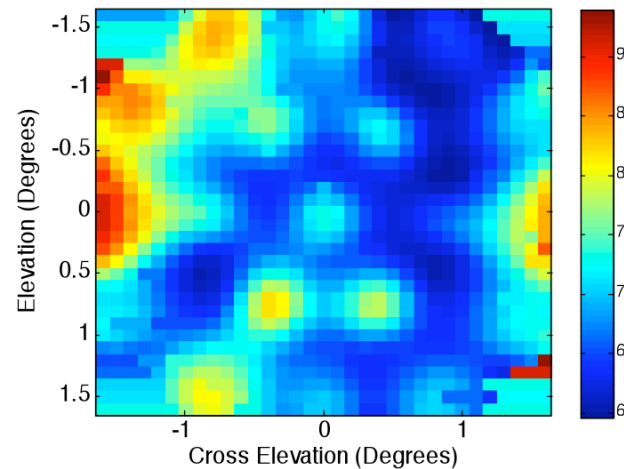


FOV $\sim \pm 1^\circ$
Defined by 1dB
sensitivity loss

Beam Aperture Efficiency



Beam T_{sys}

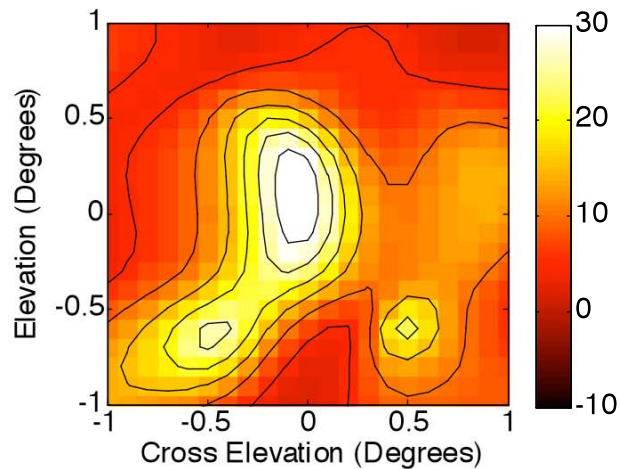




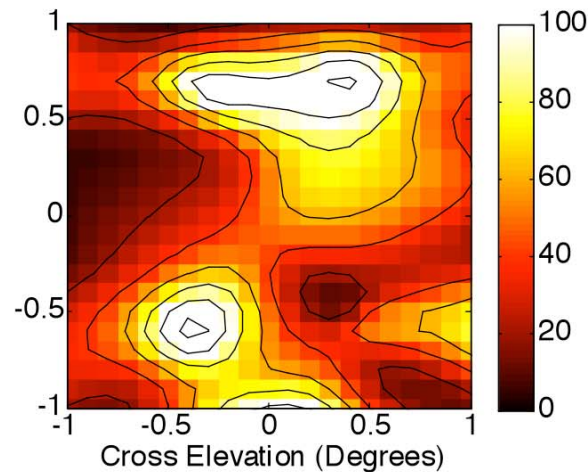
Interference Cancelation

Array enables forming tracking spatial nulls
to reject interference

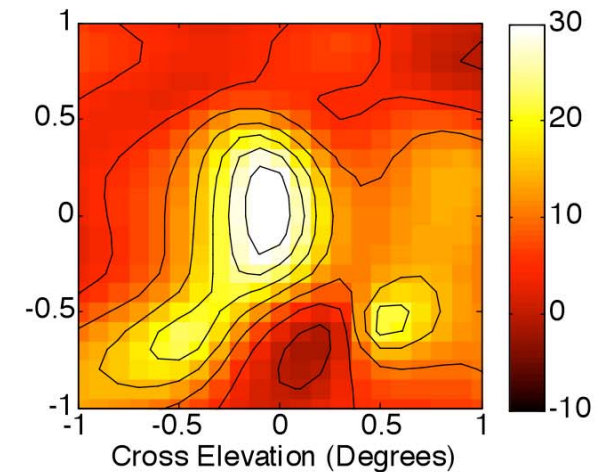
Adaptive RFI Mitigation



W3OH, no RFI



RFI corrupted image
(moving function generator
and antenna on the ground)



Adaptive spatial filtering,
Subspace projection algorithm

Challenges for Astronomical Adaptive Array RFI Canceling



- Beampattern nulls must be deep to drive an interferer *well* below the noise floor to reveal the SOI.
- Low INR interferers are hard to cancel, can't accurately estimate interference parameters.
Conventional block update cancellation null depth is limited by:
 - Sample estimation error in $\hat{\mathbf{R}}_{\text{int},k}$.
 - Subspace smearing motion within an integration (STI) window.
 - Subspace Partitioning errors (signal-noise-interference overlap, bias).
- **Solution:**
 - Fit interference $\hat{\mathbf{R}}_{\text{int},k}$ to matrix polynomial model over many STIs.
 - Better estimates of $\hat{\mathbf{R}}_{\text{int},k}$ yield deeper cancellation nulls!

Conventional Subspace Projection (SSP)



- Zero-forcing method forms deeper nulls than many array cancellers
- At k th STI, form an orthogonal projection matrix for the interferer(s):
 - Sample STI covariance estimate:

$$\hat{\mathbf{R}}_k = \frac{1}{N} \sum_{n=0}^{N-1} \mathbf{v}[n + kN] \mathbf{v}^H[n + kN] \quad \text{for } k\text{th STI of length } N$$

- Partition eigenspace. Largest eigenvalues(s) correspond to interference.

$$\hat{\mathbf{R}}_k [\mathbf{U}_{\text{int}} \mid \mathbf{U}_{\text{sig+noise}}] = [\mathbf{U}_{\text{int}} \mid \mathbf{U}_{\text{sig+noise}}] \mathbf{\Lambda}$$

- Form projection matrix:

$$\mathbf{P}_k = \mathbf{I} - \mathbf{U}_{\text{int}} \mathbf{U}_{\text{int}}^H$$

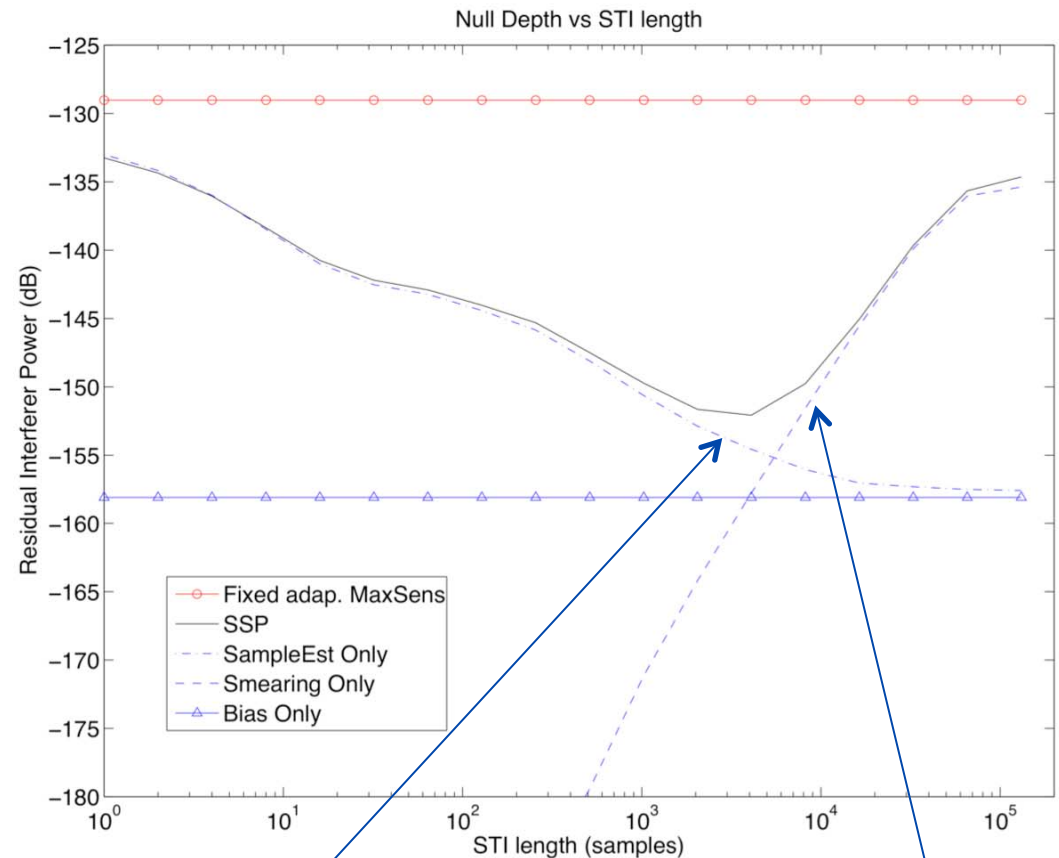
- Compute weights and beamform:

$$\mathbf{w}_{\text{SSP},k} = \mathbf{P}_k \mathbf{w}_{\text{nominal}}$$

Conventional SSP Simulation Results



- 7-element PAF on 20m reflector, 0.43f/D
- Correlated spillover noise, mutual coupling, modeled 33K Ciao Wireless LNAs.
- Measured array element radiation patterns.
- Physical Optics, full 2D integration over reflector.
- Moving point interferer
 - Average element INR: -5.01 dB.
 - Motions covers 20 – 21.8° AZ and 44 – 45.8° EL, 2.0° / sec.
 - Traverses 3 sidelobes of boresight beam.
- 291ksamp/sec, 0.9 seconds of data.



Subspace estimation error due to sample noise, i.e. null depth with no motion.

Subspace smearing error due to motion, i.e. null depth with no sample estimation error.



Low-order Parametric Model SSP

- Fit STI covariances to a polynomial in time.
 - Beamformer weights can be updated at every time sample, not just once per STI.
 - Use entire data window to fit polynomial → less sample estimation error.
 - Exploit knowledge that physical motion yields smooth progression of $\mathbf{R}_{\text{int}}[n]$.

$$\tilde{\mathbf{R}}_{\text{int}}(t, \mathbf{C}) = \mathbf{a}_{\text{poly}}(t, \mathbf{C}) \mathbf{a}_{\text{poly}}^H(t, \mathbf{C}) \Big|_{t=nT_s}, \text{ where } \mathbf{C} = [\mathbf{c}_0 \cdots \mathbf{c}_r],$$

$$\mathbf{a}_{\text{poly}}(t, \mathbf{C}) = \mathbf{c}_0 + \mathbf{c}_1 t + \cdots + \mathbf{c}_r t^r, \text{ and } T_s = \text{sample period}$$

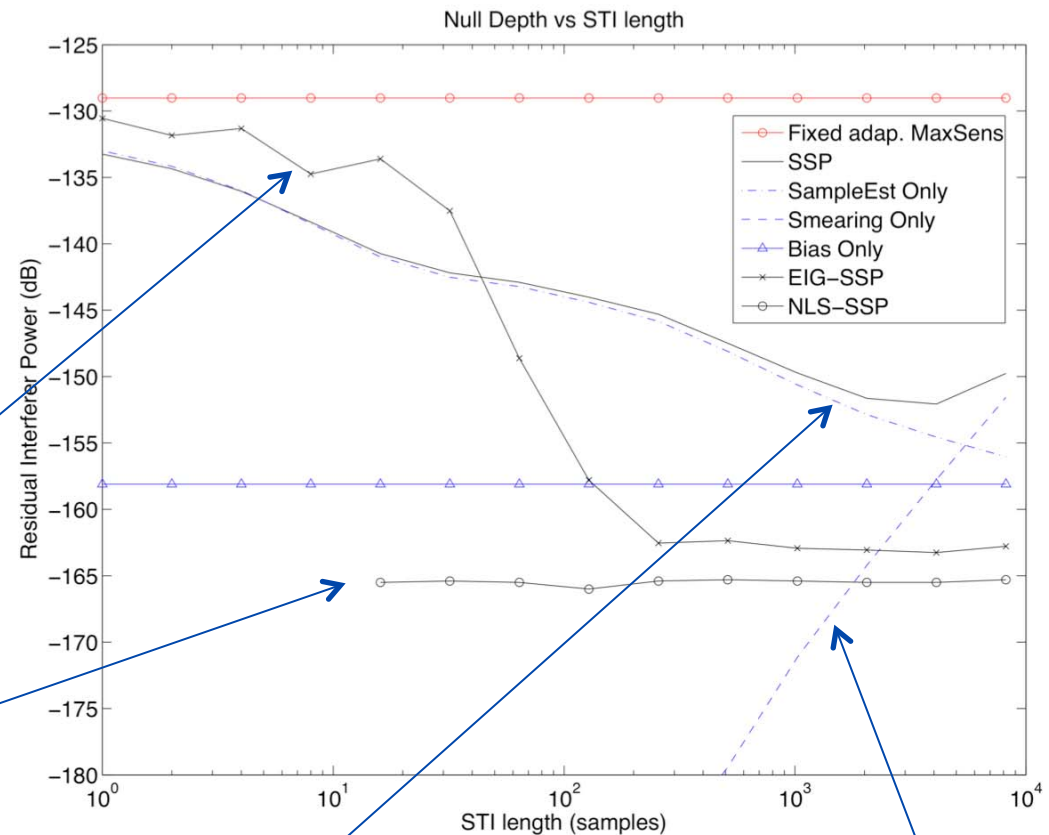
- Minimize the squared error between STI sample covariances and the polynomial model:

$$\mathbf{C}_{\text{LS}} = \arg \min_{\mathbf{C}} \sum_{k=1}^K \left\| \hat{\mathbf{R}}_k - \tilde{\mathbf{R}}_{\text{int}}(t_k, \mathbf{C}) \right\|_F^2, \text{ where } t_k = kNT_s$$

Polynomial-augmented SSP Results



- Polynomial order = 8.
- 13.4dB improvement over conventional SSP.
- EIG-SSP improves null depth by 11dB; NLS-SSP improves null depth by another 2.4dB.
- EIG-SSP requires enough averaging to get a good set of eigenvectors for regression.
- NLS-SSP computationally more difficult as STIs get shorter, but works over a wider range of STI lengths.



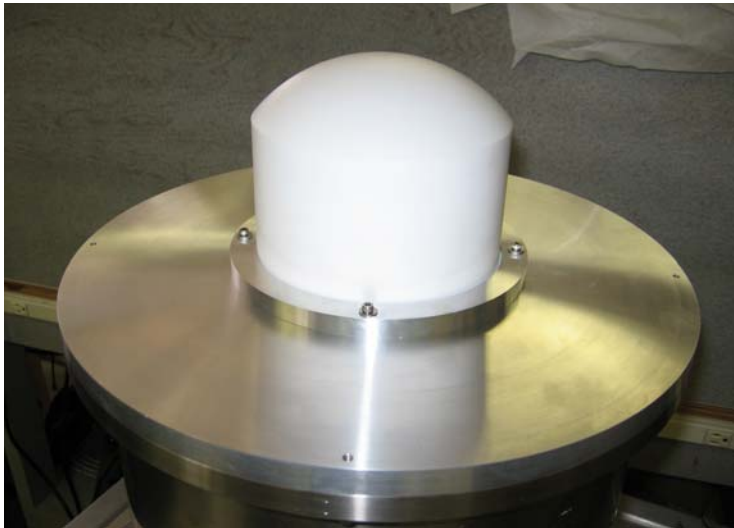
Subspace estimation error due to sample noise, i.e. null depth with no motion.

Subspace smearing error due to motion, i.e. null depth with no sample estimation error.

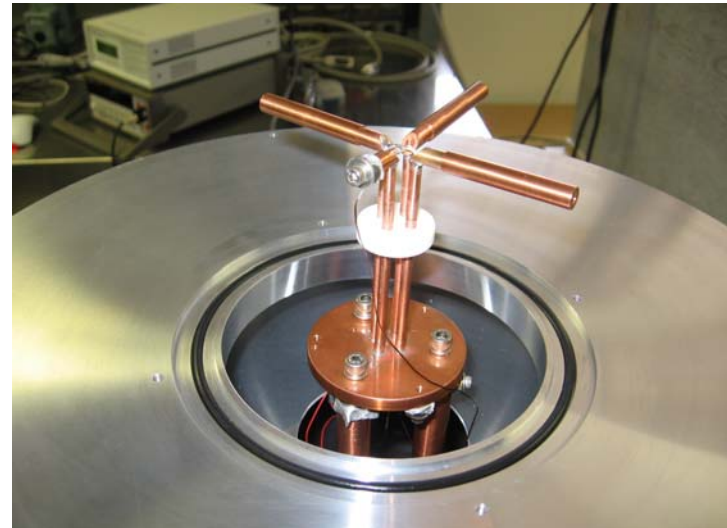
Array Cryogenic Cooling



Dielectric dome acts as both vacuum and RF window.



L-band dual-polarization dipole on a 15K cooling station with temperature sensors.



- Most groups plan room temperature arrays, $T_{\text{sys}} \approx 66\text{K}$.
- Logistics, materials, and heat loads are daunting.
- NRAO Green Bank is studying array cooling.
- LNA & antenna with LNA cryo options are being investigated, $T_{\text{sys}} \approx 33\text{K}$.
- For a fixed source flux detection level, a modest sized cryo-cooled array may yield better survey speed than a larger high temp array.



Conclusions and Future Work

- First demonstration of high sensitivity imaging with a PAF.
- Practical calibration and beamforming methods.
- Sensitivity, system temperature efficiency, and realized field of view match model predictions to within expected accuracy.
- Demonstration of true elevation tracking sensitivity optimization.
- Significant progress towards a truly usable adaptive PAF canceller.
- Future work:
 - Dual pol, 37 element array.
 - Real time distributed data acquisition, 5 MHz instantaneous BW.
 - Design PAF for field of view average optimal LNA noise match to reduce mutual coupling noise penalty.
 - Cryogenically cooled arrays.
 - Science-ready PAFs for Green Bank Telescope, Arecibo, SKA.
 - Apply polynomial assisted SSP to real data sets.

Cygnus X Region at 1600 MHz

